

# Node-Pore Sensing Enables Label-Free Surface-Marker Profiling of Single Cells

## Supporting Information

Karthik R. Balakrishnan,<sup>†</sup> Jeremy C. Whang,<sup>†,1</sup> Richard Hwang,<sup>†,2</sup> James H. Hack,<sup>†,3</sup> Lucy A. Godley,<sup>‡</sup> and Lydia L. Sohn,<sup>\*,†</sup>

<sup>†</sup> Department of Mechanical Engineering, University of California, Berkeley, 5118 Etcheverry Hall, Mail Stop 1740, Berkeley, CA, 94720-1740, USA.

<sup>‡</sup> Section of Hematology/Oncology, Department of Medicine, The University of Chicago, Chicago, IL 60637, USA.

Present Addresses:

<sup>1</sup>Dept. of Biomedical Engineering, Tulane University, New Orleans, Louisiana 70118

<sup>2</sup>The Carol Franc Buck Breast Care Center, University of California, San Francisco, CA 94143

<sup>3</sup>Dept. of Materials Science & Engineering, University of Delaware, Newark, Delaware 19716

## Table of Contents

Fig. S-1. Isotype control node-pore testing with transit-time cutoff determination.

Fig. S-2. FCM forward-scatter and side-scatter plots and an overlay fluorescence histogram of NB4 cells.

Fig. S-3. FCM forward-scatter and side-scatter plots and an overlay fluorescence histogram of AP-1060 cells.

Fig. S-4. FCM forward-scatter and side-scatter plots and an overlay fluorescence histogram of a 1:1 NALM-1/AP-1060 cell mixture.

Fig. S-5. Propidium Iodide testing for cell viability post screening with the node-pore.

Fig. S-6. Isotype control node-pore testing of AML patient bone-marrow samples for transit-time cutoff determination.

Fig. S-7. FCM of AML Patient 1 bone-marrow sample.

Fig. S-8. FCM of AML Patient 2 bone-marrow sample.

Fig. S-9. FCM of AML Patient 3 bone-marrow sample.

Fig. S-10. Model of fluid flow through a node-pore device.

Table S-1. Antibody details for FCM and NPS of cell lines.

Table S-2.  $\chi^2$  test comparing NPS with FCM for cell lines.

Table S-3. Antibody details for FCM and NPS of AML patient samples.

Table S-4.  $\chi^2$  test comparing NPS with FCM on AML patient samples.

### *Device functionalization*

Prior to antibody functionalization, glass substrates with pre-defined electrodes were cleaned using a modified RCA-1 clean protocol<sup>1, 2</sup> to remove any organic contaminants on the substrate surface, while still preserving the integrity of the electrodes. Substrates were placed in a 1:10 ammonium hydroxide (NH<sub>4</sub>OH) : 18 MΩ deionized (DI) water solution and heated at 150°C for 10 minutes. 30% Hydrogen peroxide (H<sub>2</sub>O<sub>2</sub>) was then added to the solution (for a final mixture ratio of 1:1:10 H<sub>2</sub>O<sub>2</sub> : NH<sub>4</sub>OH : DI water). After 10 minutes, the glass substrates were removed, rinsed with DI water and methanol (MeOH), and subsequently dried with dry nitrogen gas. To functionalize the individual sections of the node pore with antibodies, temporary polydimethylsiloxane (PDMS) microchannels, whose widths corresponded to the length of the region between the nodes, were fabricated using soft lithography and then aligned and clamped orthogonal to what would be the final node-pore device (Fig. 1B). A 1:50 APTES ((3-Aminopropyl)triethoxysilane, Sigma-Aldrich) : acetone mixture was subsequently injected into each temporary microchannel, and the entire device was incubated in a humid chamber for 10 minutes. The channels were then flushed with acetone and subsequently dried with dry nitrogen gas. Next, acetone was flushed through the channels, and the glass substrates were heated at 100°C for 30 minutes. After cooling, 10 mg/mL of Sulfo EGS crosslinker (Pierce) in phosphate buffered saline (PBS) solution was injected into the devices and incubated for 1 hour in a humid chamber. After the devices were flushed with PBS, 1 mg/mL of Protein G (Pierce) in PBS was injected into the microchannels and incubated overnight at 4°C. After incubation, PBS was again injected into the channels. Finally, antibodies at a saturating concentration (Table S-1) were injected into the microchannels and incubated overnight at 4°C. Prior to testing, the devices were flushed with PBS, and the node-pore mold, fabricated using soft lithography, was aligned and clamped to the functionalized substrate.

### *Node-pore fabrication*

The node-pore platform consisted of a PDMS mold and a glass substrate. Electrodes and contact pads were lithographically patterned onto the substrate using Microposit S1813 (Dow) resist. A thin film of 75/250/250 Å titanium/platinum/gold was deposited using an electron-gun evaporator. Gold etchant was used to expose the platinum layer of the electrodes while keeping the contact pads coated with gold. Completed electrodes and contact pads enabled a four-terminal measurement of the current across the node-pore. Standard lithography was used to create SU-8 photoresist negative-relief masters of the node-pore design on polished silicon wafers. De-gassed PDMS (Sylgard 184) (10:1 pre-polymer : curing agent) was dispensed onto the masters and cured at 80°C for an hour. Prior to measurement, a slab of PDMS with the embedded node-pore was cut. A 16 G syringe needle was used to core inlet and outlet ports. The temporary PDMS channels used for functionalization were fabricated in a similar manner.

### *Positive cell-surface marker expression cutoff determination for cell lines*

To account for non-specific interactions between cell-surface antigens and the functionalized isotype-control antibodies in the node-pores, we employed a normalized transit-time threshold value to determine which cells in a sample were positive for a particular surface marker. We determined this threshold by screening cells in node-pores consisting of two consecutive segments functionalized with IgG1 isotype control antibody (Abcam, see Table S-1

for the saturating concentration of antibody utilized) (Fig. S-1A). We normalized each cell's transit time as follows,

$$\tau_{\text{norm}} = \tau_{\text{IgG1 segment 1}} / \tau_{\text{IgG1 segment 2}} \quad \text{Eq. (1)}$$

and determined the standard deviation,  $\sigma_{\text{isotype}}$ , of the normalized transit-time distribution of all cells in a given sample. The positive-expression threshold cutoff for each sample was set to  $1+2\sigma_{\text{isotype}}$ , to account for the inherent variability in nonspecific interactions between the cells and functionalized isotype-control antibodies. Normalized transit-time distributions of NB4, AP-1060, and NALM-1/AP-1060 mixed samples are shown in Fig. S-1B (top row), with threshold cutoff values (determined to be 1.0228, 1.0250, 1.0229, respectively for each sample) denoted with a vertical dashed line.

### *Size determination*

Because the cells were comparable in size to the node-pore, cell size could be determined by the following from DeBlois and Bean<sup>3</sup>

$$\frac{\Delta I}{I} = \frac{d^3}{D^2 L} \left[ \frac{1}{1 - \left[ 0.8 \frac{d^3}{D^3} \right]} \right] \quad \text{Eq. (2)}$$

where  $I$  is the baseline current,  $\Delta I$  is the change in current magnitude caused by the cell,  $d$  is the cell diameter,  $D$  is the node-pore effective diameter, and  $L$  is the total node-pore length. Node-pore effective diameter was determined using colloids of known size (15  $\mu\text{m}$ ) for calibration. Size distributions of NB4, AP-1060, and NALM-1/AP-1060 mixed samples screened with the isotype control devices (Fig. S-1A) used for normalized transit-time threshold determination are shown in Fig. S-1B (bottom row).

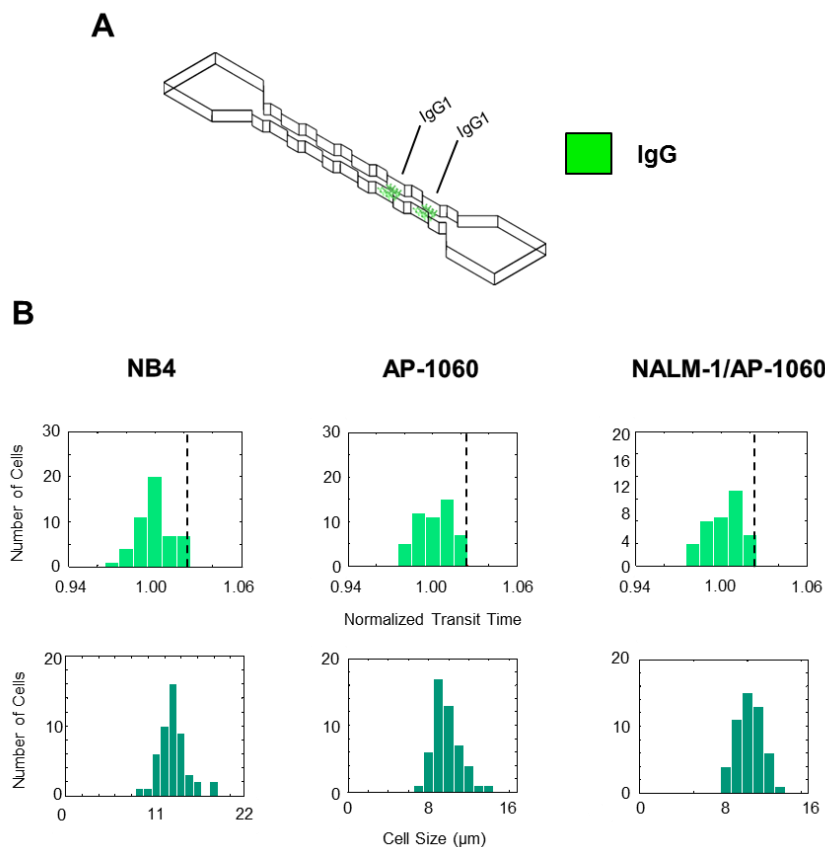


**Fig. S-1.** Isotype control node-pore testing with transit-time cutoff determination. **(A)** Schematic of a four-node-pore with two consecutive sections functionalized with IgG1 isotype control antibody. The actual device was  $18\ \mu\text{m} \times 18\ \mu\text{m}$  (H x W) with five  $1150\text{-}\mu\text{m}$  long segments separated by four nodes, each  $58\text{-}\mu\text{m}$  wide and  $50\text{-}\mu\text{m}$  long. **(B) (top row)** Data obtained by screening NB4 cells ( $10^6$  cells/mL), AP-1060 ( $2 \times 10^6$  cells/mL), and a 1:1 mixture of NALM-1 : AP-1060 cells ( $10^6$  cells/mL) with the prepared IgG1 node-pore devices. Normalized transit-time distributions of the NB4, AP-1060, and mixed NALM-1 : AP-1060 cells (top row), with the positive expression cutoffs, corresponding to  $1+2\sigma_{\text{isotype}}$ , indicated by the vertical dashed lines. We applied these cutoffs to the data shown in Figs. 2 and 3. **(bottom row)** Cell-size distribution of each sample of cells screened.

*Flow cytometry of cell lines*

Cells for FCM were prepared by first washing  $10^6$  cells/mL in PBS 1X by centrifugation at 300 g for 3 minutes and re-suspending in fresh PBS. They were then incubated with 4% formaldehyde for 15 minutes before being washed two more times with PBS and subsequently suspended in PBS with 1% bovine serum albumin (BSA, Sigma-Aldrich) and 0.1% sodium azide (Sigma-Aldrich). Cells were then incubated with primary antibody at 10  $\mu$ g/ml for 3 hours. Samples were then washed three more times with PBS before being suspended in 1% BSA and 0.1% sodium azide with secondary antibody (Alexa Fluor 488 Goat Anti-Mouse IgG) at 2  $\mu$ g/mL and stored for 90 minutes in the dark. After incubation, samples were washed three more times with PBS and finally suspended in PBS with 1% BSA and 0.1% sodium azide for FCM testing in an FC 500 Series machine (Beckman Coulter). FCM data for NB4 cells, AP-1060 cells, and the NALM-1/AP-1060 cell mixture are shown in Figs. S-2, S-3, and S-4, respectively. Antibody details are found in Table S-1.

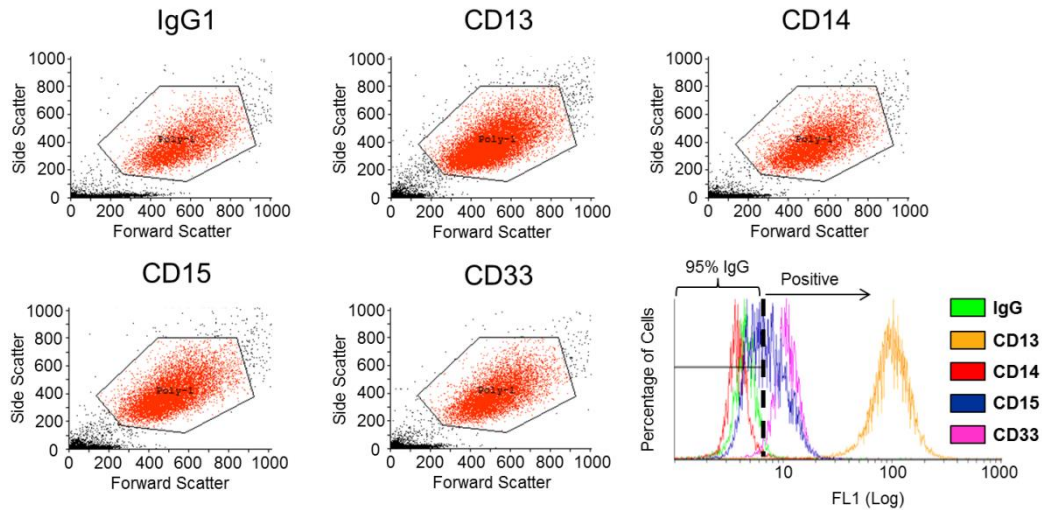


**Fig. S-2.** FCM forward-scatter and side-scatter plots and an overlay fluorescence histogram of NB4 cells. Each sample was stained with a different primary antibody (IgG1, anti-CD13 Ab., anti-CD14 Ab., anti-CD15 Ab., or anti-CD33 Ab.) and then secondary antibody (Alexa Fluor 488 Goat polyclonal Secondary Antibody to Mouse IgG). A vertical dashed line indicates 95% ( $2\sigma$ ) of the IgG sample. Cells expressing more fluorescence than this cutoff value were determined to be positive for the particular surface marker.

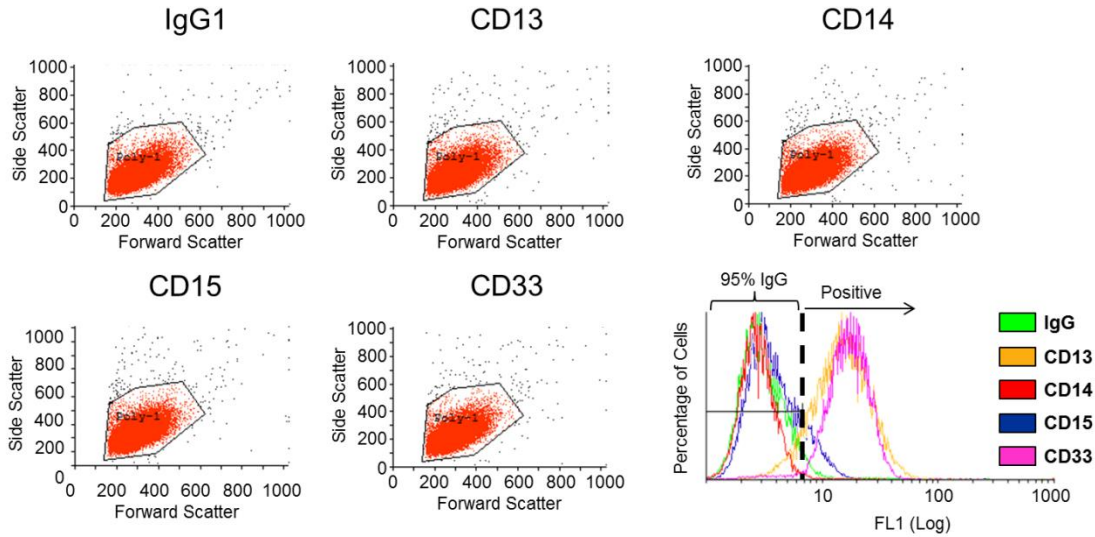


**Fig. S-3.** FCM forward-scatter and side-scatter plots and an overlay fluorescence histogram of AP-1060 cells. Each sample was stained with a different primary antibody (IgG1, anti-CD13 Ab., anti-CD14 Ab., anti-CD15 Ab., or anti-CD33 Ab.) and then secondary antibody (Alexa Fluor 488 Goat polyclonal Secondary Antibody to Mouse IgG). A vertical dashed line is shown to indicate 95% ( $2\sigma$ ) of the IgG sample. Cells expressing more fluorescence than this cutoff value were determined to be positive for the particular surface marker.

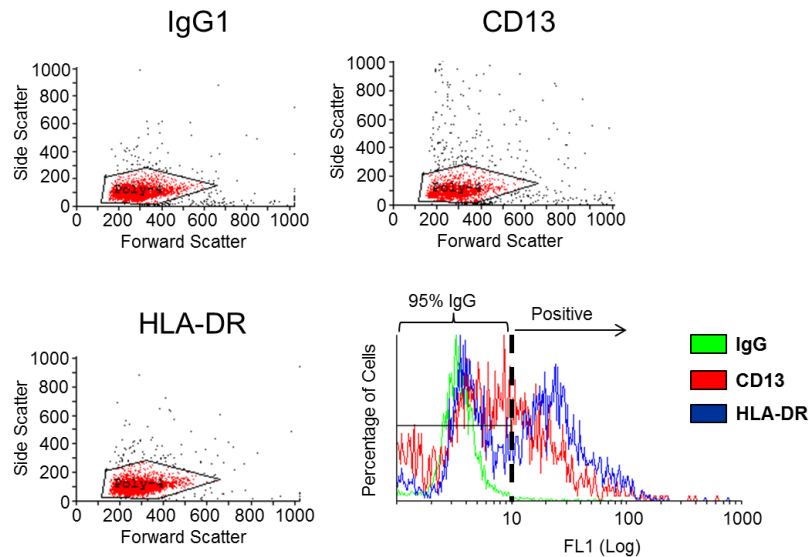


**Fig. S-4.** FCM forward-scatter and side-scatter plots and an overlay fluorescence histogram of a 1:1 NALM-1/AP-1060 cell mixture. Each sample was stained with a different primary antibody (IgG1, anti-CD13 Ab., or anti-HLA-DR Ab.) and then secondary antibody (Alexa Fluor 488 Goat polyclonal Secondary Antibody to Mouse IgG). A vertical dashed line is shown to indicate 95% ( $2\sigma$ ) of the IgG sample. Cells expressing more fluorescence than this cutoff value were determined to be positive for the particular surface marker.

**Table S-1.** Antibody details for FCM and NPS of cell lines.

Antibody (Abcam)	Clone	Stock Concentration	Flow Cytometry Concentration	Node-pore Substrate Concentration
Anti-CD13	WM15	1 mg/mL	10 µg/mL	1 mg/mL
Anti-CD14	2Q1233	1 mg/mL	10 µg/mL	1 mg/mL
Anti-CD15	4E10	1 mg/mL	10 µg/mL	1 mg/mL
Anti-CD33	WM53	1 mg/mL	10 µg/mL	1 mg/mL
Anti-HLA DR	TAL 1B5	1 mg/mL	10 µg/mL	1 mg/mL
Mouse IgG1 Monoclonal	NCG01	1 mg/mL	10 µg/mL	1 mg/mL
Goat Anti-Mouse IgG H&L (Alexa Fluor 488)	N/A	2 mg/mL	2 µg/mL	N/A

*Statistical analysis to compare screening of cell lines with NPS and FCM*

We employed a  $\chi^2$  test,

$$\chi^2 = \sum_{i=1}^n \frac{(O_i - E_i)^2}{E_i} \quad \text{Eq. (3)}$$

to determine whether there were any statistically significant differences between NPS and FCM results. The observed values,  $O_i$ , were the number of cells NPS detected as positive for a particular surface marker in a sample. The expected values,  $E_i$ , were the number of cells expected to be positive in the same sample based on the percentages FCM obtained for each surface marker; these percentages were applied to the total number of cells screened with the NPS device. Table S-2 shows the  $\chi^2$  values of the NB4, AP-1060, and AP-1060/NALM-1 mixture samples. For a p-value=0.05,  $\chi^2=3.841$ . Thus, the only statistically significant differences between FCM and NPS results were those corresponding to the screening of CD14 and CD33 on AP-1060 cells. As discussed in the main text, the discrepancy between the two methods for CD14 screening was exaggerated due to the fact that a small number of cells were expected to express this marker (i.e.,  $E_i$  was extremely small, leading to a high  $\chi^2$  value even with a small deviation,  $O_i - E_i$ , in the observed value). In general, utilizing a redundant antibody patterning as had been done for the screening of the AP-1060/NALM-1 mixture, would greatly reduce the differences between the two methods.

**Table S-2.**  $\chi^2$  test with  $p=0.05$  comparing NPS with FCM for cell lines.

Surface Antigen	NB4 $\chi^2$	AP-1060 $\chi^2$	AP-1060/NALM-1 Mixture $\chi^2$
CD13	0.294	0.526	0.0817
CD14	2.223	5.868	N/A
CD15	1.274	2.196	N/A
CD33	1.300	5.568	N/A
HLA-DR	N/A	N/A	0.220

### Viability testing

To demonstrate that NPS does not damage cells during the screening process, we used Propidium Iodide (PI) to determine the number of dead cells post-screening. We collected AP-1060 cells from the outlet port of the node-pore devices after screening (Fig. S-5A) and incubated these cells with PI solution (1.0 mg/mL, Life Technologies) for 10 minutes in a 1:100 PI : cell media volume ratio. We then used fluorescence intensity to identify dead cells (Fig. S-5B). Of the 315 cells we analyzed, only 7 cells (i.e. 2.2%) showed high levels of fluorescence. Thus, greater than 97% of cells screened with the node-pore devices remained viable. As a control, we performed a viability test on cells that we did not screen with the node-pore devices. We found that 96% of these control cells remained viable. Thus, we can safely conclude that our node-pore method does not damage cells during the screening process.

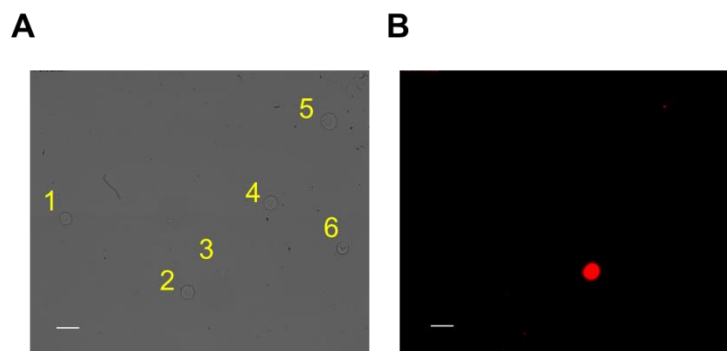


**Fig. S-5.** Propidium Iodide testing for cell viability post screening with the node-pore. **(A)** Bright-field image of six AP-1060 cells that were collected from the output of a node-pore device and stained with PI. **(B)** Fluorescent image of the same 6 cells show that only cell 3 (red) had died; the rest remained viable after being screened in the node-pore device. Scale bar, 20  $\mu\text{m}$  (A and B).



*Positive surface-marker expression cutoff determination for AML patient bone-marrow samples*

To establish the normalized transit-time threshold value, which we then use to determine whether a blast cell is positive for a particular surface marker, we screened a sample of each patient's cells in node-pores that had isotype-control patterned segments. Because the anti-HLA-DR antibody used in these experiments had a different isotype control than that of all the other antibodies (IgG2 vs. IgG1), the node-pores consisted of two consecutive segments that were functionalized with one isotype control antibody and two segments functionalized with the other isotype control antibody, as shown in Fig. S-6A. We analyzed only those cells that were greater than 12  $\mu\text{m}$  and normalized their transit times as follows,

$$\tau_{\text{norm, IgG1}} = \tau_{\text{IgG1 segment 1}} / \tau_{\text{IgG1 segment 2}} \quad \text{Eq. (4)}$$

$$\tau_{\text{norm, IgG2}} = \tau_{\text{IgG2 segment 1}} / \tau_{\text{IgG2 segment 2}} \quad \text{Eq. (5)}$$

For each patient sample, we determined the standard deviation of each normalized transit-time distribution,  $\sigma_{\text{IgG1}}$  and  $\sigma_{\text{IgG2}}$ , and as before, set the positive-expression threshold cutoff to be  $1+2\sigma_{\text{isotype}}$ , thereby taking into account the inherent variability in nonspecific interactions between the cells and functionalized isotype-control antibodies. Normalized transit-time distributions are shown in Fig. S-6B, with threshold cutoff values for each patient sample denoted with a vertical dashed line. Threshold cutoff values were determined to be 1.0580, 1.0609, 1.0492 for IgG1, and 1.0514, 1.0460, 1.0467 for IgG2 for Patient 1, 2, and 3, respectively.

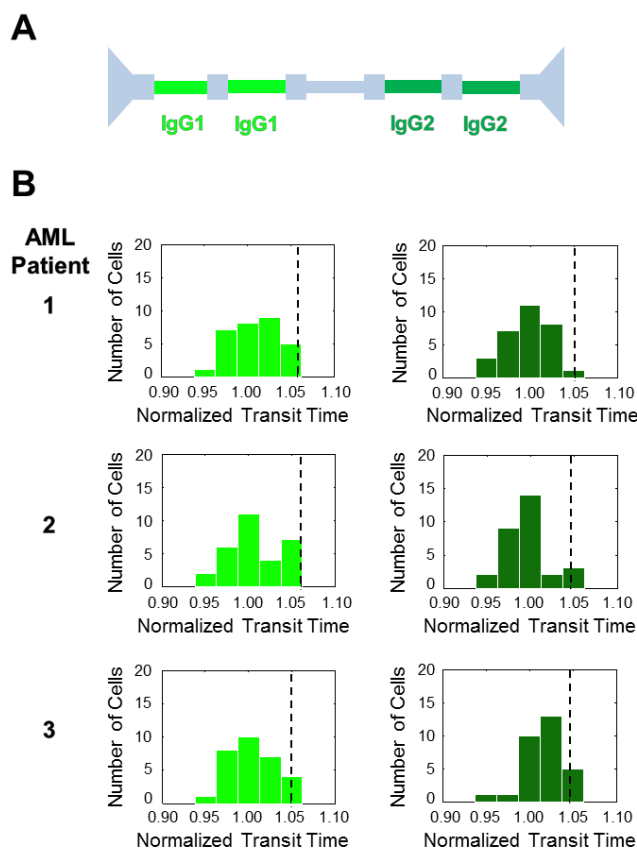


**Fig. S-6.** Isotype-control node-pore testing of AML patient bone-marrow samples for transit-time cutoff determination. **(A)** Schematic of a four-node pore with two consecutive segments functionalized with IgG1 isotype-control antibody and two consecutive segments functionalized with IgG2 isotype-control antibody. The device dimensions were  $25\mu\text{m} \times 25\mu\text{m}$  ( $H \times W$ ) with five  $1150\mu\text{m}$  long segments separated by four nodes, each  $65\mu\text{m} \times 50\mu\text{m}$  ( $W \times L$ ). **(B)** Normalized transit-time distributions for IgG1 (left) and IgG2 (right) for all three patient samples are shown, and the positive-expression cutoffs, corresponding to  $1+2\sigma_{\text{isotype}}$ , are indicated by the vertical dashed lines.

#### *AML patient bone-marrow sample flow cytometry*

Bone marrow samples for FCM were prepared by first washing the cells in PBS (1X) by centrifugation at 300 g for 3 minutes and re-suspending in fresh PBS. Cells were then incubated with 4% formaldehyde for 15 minutes before being washed two more times with PBS and subsequently suspended in PBS with 1% bovine serum albumin (BSA, Sigma-Aldrich) and 0.1% sodium azide (Sigma-Aldrich). They were then incubated in the dark with primary antibody at 4  $\mu\text{g}/\text{ml}$  for 30 minutes. After incubation, cells were washed three more times with PBS and finally suspended in PBS with 1% BSA and 0.1% sodium azide at  $10^6$  cells/mL for FCM testing in an FC 500 Series machine (Beckman Coulter). FCM data for the samples from Patient 1, 2, and 3 are shown in Figs. S-7, S-8, and S-9, respectively. Antibody details are found in Table S-3.

**Table S-3.** Antibody details for FCM and NPS of AML patient samples.

<b>Antibody (Biolegend)</b>	<b>Clone</b>	<b>Stock Concentration</b>	<b>Flow Cytometry Concentration</b>	<b>Node-pore Substrate Concentration</b>
Anti-CD13	WM15	0.5 mg/mL	N/A	0.5 mg/mL
Anti-HLA DR	L243	0.5 mg/mL	N/A	0.5 mg/mL
Anti-CD34	581	0.5 mg/mL	N/A	0.5 mg/mL
Anti-CD45	HI30	0.5 mg/mL	N/A	0.5 mg/mL
Mouse IgG1, $\kappa$	MOPC-21	0.5 mg/mL	N/A	0.5 mg/mL
Mouse IgG2a, $\kappa$	MOPC-173	0.5 mg/mL	N/A	0.5 mg/mL
PE Anti-CD13	WM15	0.2 mg/mL	4 $\mu$ g/mL	N/A
PE Anti-HLA DR	L243	0.02 mg/mL	4 $\mu$ g/mL	N/A
Alexa Fluor 488 Anti-CD34	581	0.2 mg/mL	4 $\mu$ g/mL	N/A
PerCP Anti-CD45	HI30	0.2 mg/mL	4 $\mu$ g/mL	N/A
PE Mouse IgG1, $\kappa$	MOPC-21	0.2 mg/mL	4 $\mu$ g/mL	N/A
PerCP Mouse IgG1, $\kappa$	MOPC-21	0.2 mg/mL	4 $\mu$ g/mL	N/A
Alexa Fluor 488 Mouse IgG1, $\kappa$	MOPC-21	0.2 mg/mL	4 $\mu$ g/mL	N/A
PE Mouse IgG2a, $\kappa$	MOPC-173	0.2 mg/mL	4 $\mu$ g/mL	N/A

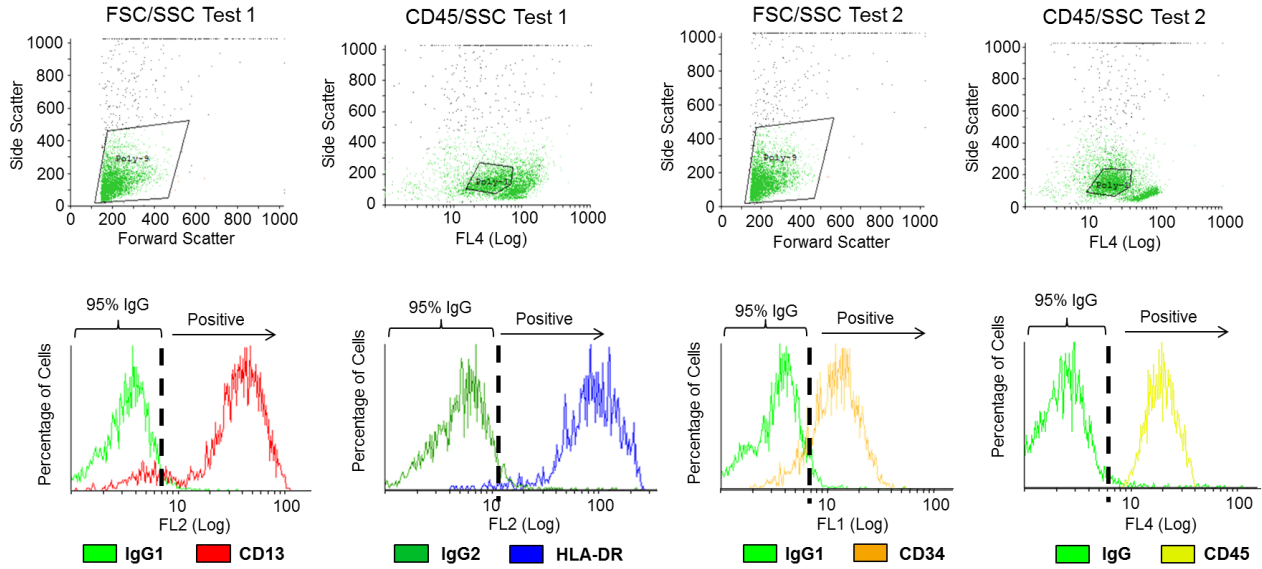


**Fig. S-7.** FCM of AML Patient 1 bone-marrow sample. Two tests were performed, with each test involving staining with anti-CD34 antibody, anti-CD45 antibody, and either anti-CD13 or anti-HLA-DR antibody. Forward scatter/side scatter plots and CD45/side scatter plots are shown for both tests (top row). The CD45/side scatter plots were used to gate for the blast-cell population. Histograms showing fluorescence compared to isotype-control antibody staining are shown with vertical dashed lines indicating 95% ( $2\sigma$ ) of the control samples, which was used as a positive cutoff.

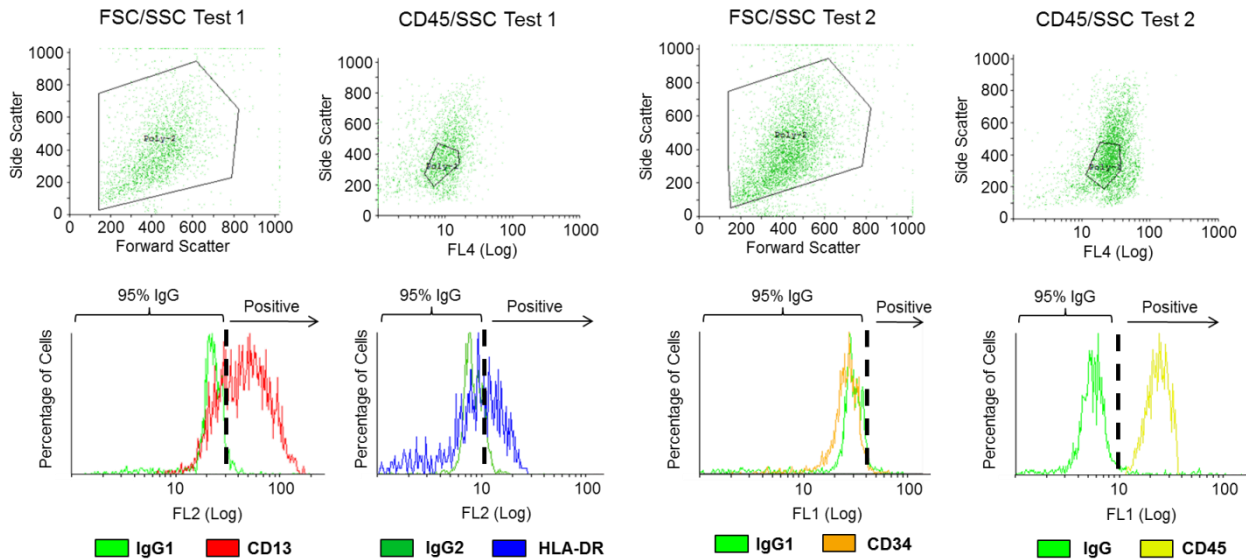


**Fig. S-8.** FCM of AML Patient 2 bone-marrow sample. Two tests were performed with each test involving staining with anti-CD34 antibody, anti-CD45 antibody, and either anti-CD13 or anti-HLA-DR antibody. Forward scatter/side scatter plots and CD45/side scatter plots are shown for both tests (top row). The CD45/side scatter plots were used to gate for the blast cell population. Histograms showing fluorescence compared to isotype-control antibody staining are shown with vertical dashed lines indicating 95% ( $2\sigma$ ) of the control samples, which was used as a positive cutoff.

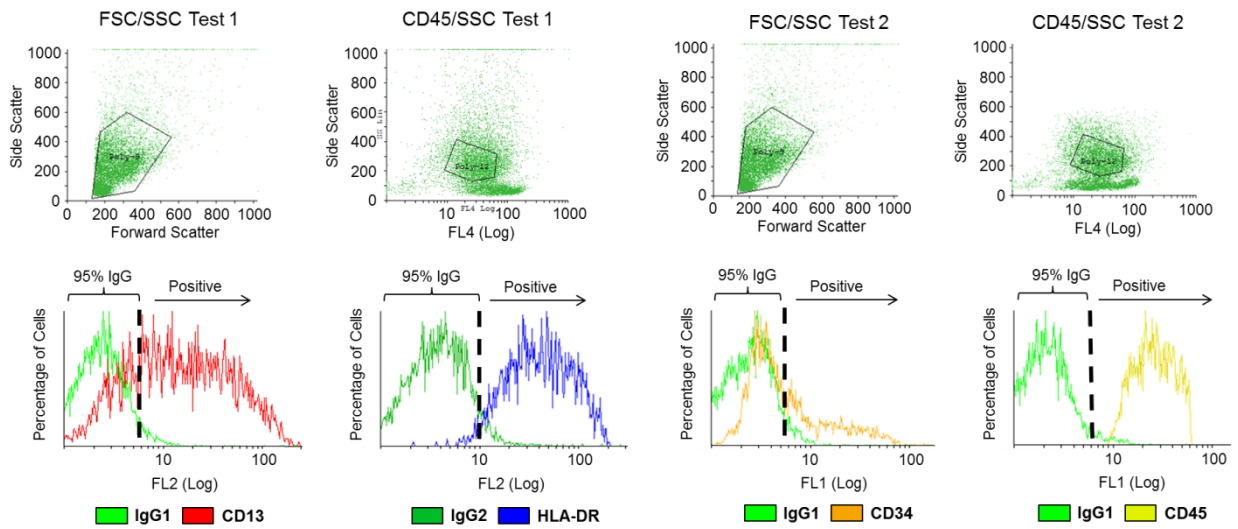


**Fig. S-9.** FCM of AML Patient 3 bone-marrow sample. Two tests were performed with each involving staining with anti-CD34 antibody, anti-CD45 antibody, and either anti-CD13 or anti-HLA-DR antibody. Forward scatter/side scatter plots and CD45/side scatter plots both tests (top two rows). The CD45/side scatter plots were used to gate for the blast population. Histograms for both blast populations showing fluorescence compared to isotype-control antibody staining are shown with vertical dashed lines indicating 95% ( $2\sigma$ ) of the control samples, which was used as a positive cutoff.

*Statistical analysis of patient bone marrow sample testing*

We employed a  $\chi^2$  test with  $p=0.05$  on the patient bone-marrow samples to determine whether there were any statistically significant differences between NPS and FCM results. Table S-4 shows the  $\chi^2$  values of all three patient samples. The only statistically significant difference between FCM and NPS was the screening of CD34 for Patient 2. In this specific case, the high  $\chi^2$  value between the two methods was exaggerated due to the fact that only a small number of cells were expected to express this marker; however both methods were consistent in finding minimal expression overall.

**Table S-4.**  $\chi^2$  test with  $p=0.05$  comparing NPS with FCM on AML patient samples.

Surface Antigen	Patient 1 $\chi^2$	Patient 2 $\chi^2$	Patient 3 $\chi^2$
CD13	0.008	1.423	2.661
HLA-DR	1.163	2.711	3.456
CD34	0.132	27.445	0.080

### Fluid modeling

We utilized COMSOL Multiphysics to model the flow through the node-pore. The device modeled had the same dimensions of the four-node devices used to screen the cells: 18  $\mu\text{m}$  x 18  $\mu\text{m}$  (H x W) with five 1150  $\mu\text{m}$  long segments separated by four nodes, each 58  $\mu\text{m}$  wide and 50  $\mu\text{m}$  long. We used an input pressure of 0.3 kPa and flow was modelled as water at room temperature (25 C). The fluid density used was 999.6  $\text{kg}/\text{m}^3$  and the dynamic viscosity was  $100 \times 10^{-5}$  Pa s. The maximum mesh element size was 4.5  $\mu\text{m}$ , and the mesh used two boundary layers with thickness 1.125  $\mu\text{m}$  and 1.350  $\mu\text{m}$ . The flow velocity (Fig. S-10), and thus cell velocity, through the node-pore significantly decreases through each node, effectively “resetting” the velocity of each cell before each measurement region.

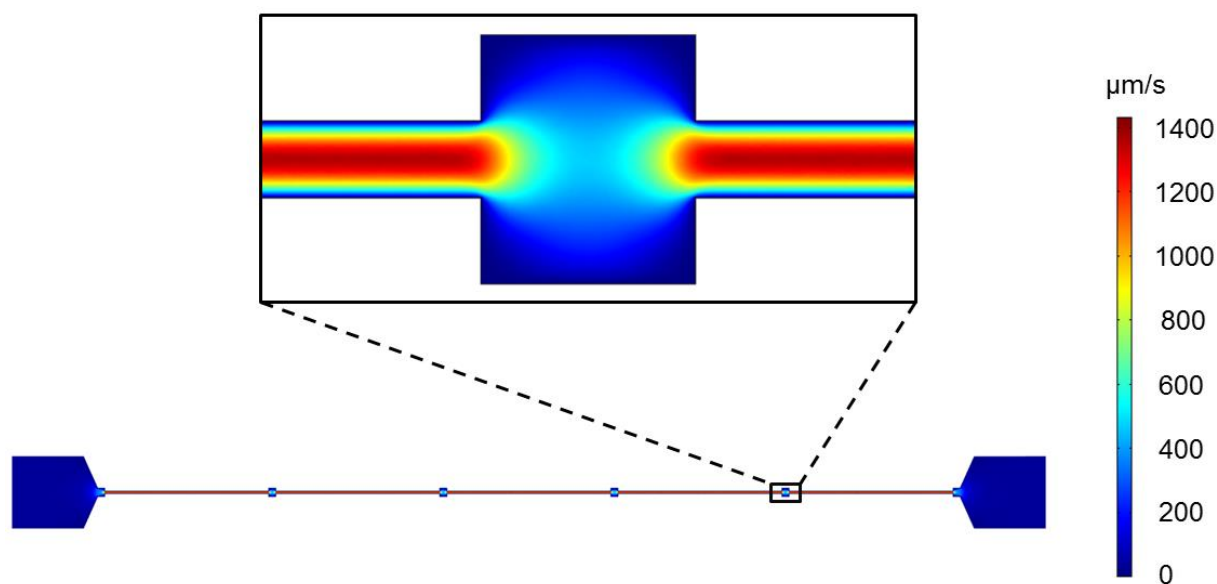


**Fig. S-10.** Model of fluid flow through a node-pore device. Fluid flow slows down significantly in each node, allowing for cell velocities to “reset” in between each measurement region, independent of antibody interaction or lack of interaction in the region before each node. The colored scale indicates the values for the velocity profile measured. Experimentally, this is confirmed in Figs. S-1 and S-6, in which there is a tight distribution of the normalized IgG1 transit time histograms centered at one, indicating that the results are not dependent on the placement of isotype control within the device.

## References

1. W. Kern and D. A. Puotinen, *RCA Review*, 1970, **31**, 187.
2. O. A. Saleh, Ph.D., Princeton University, 2003.
3. R. W. Deblois, C. P. Bean and R. K. Wesley, *Journal of Colloid and Interface Science*, 1977, **61**, 323-335.